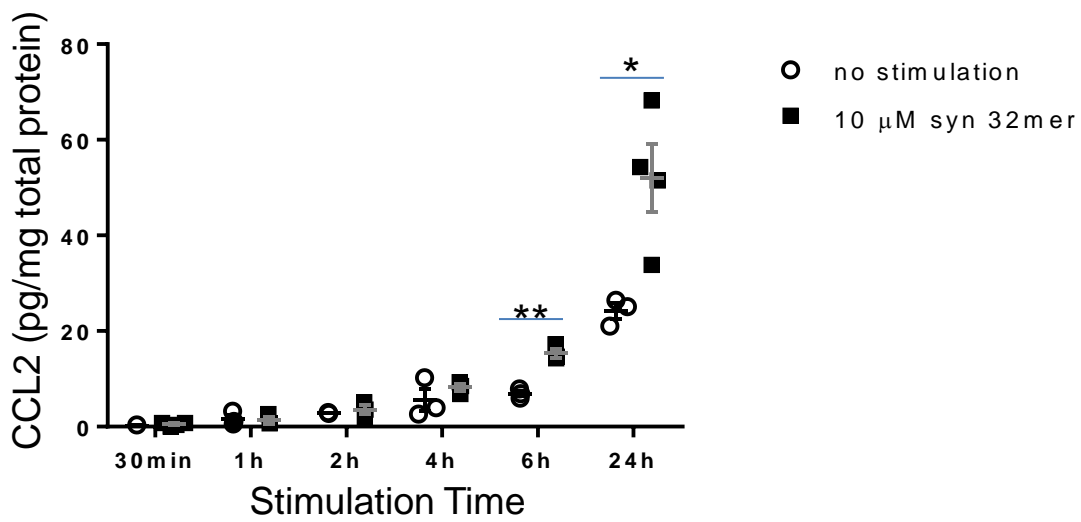
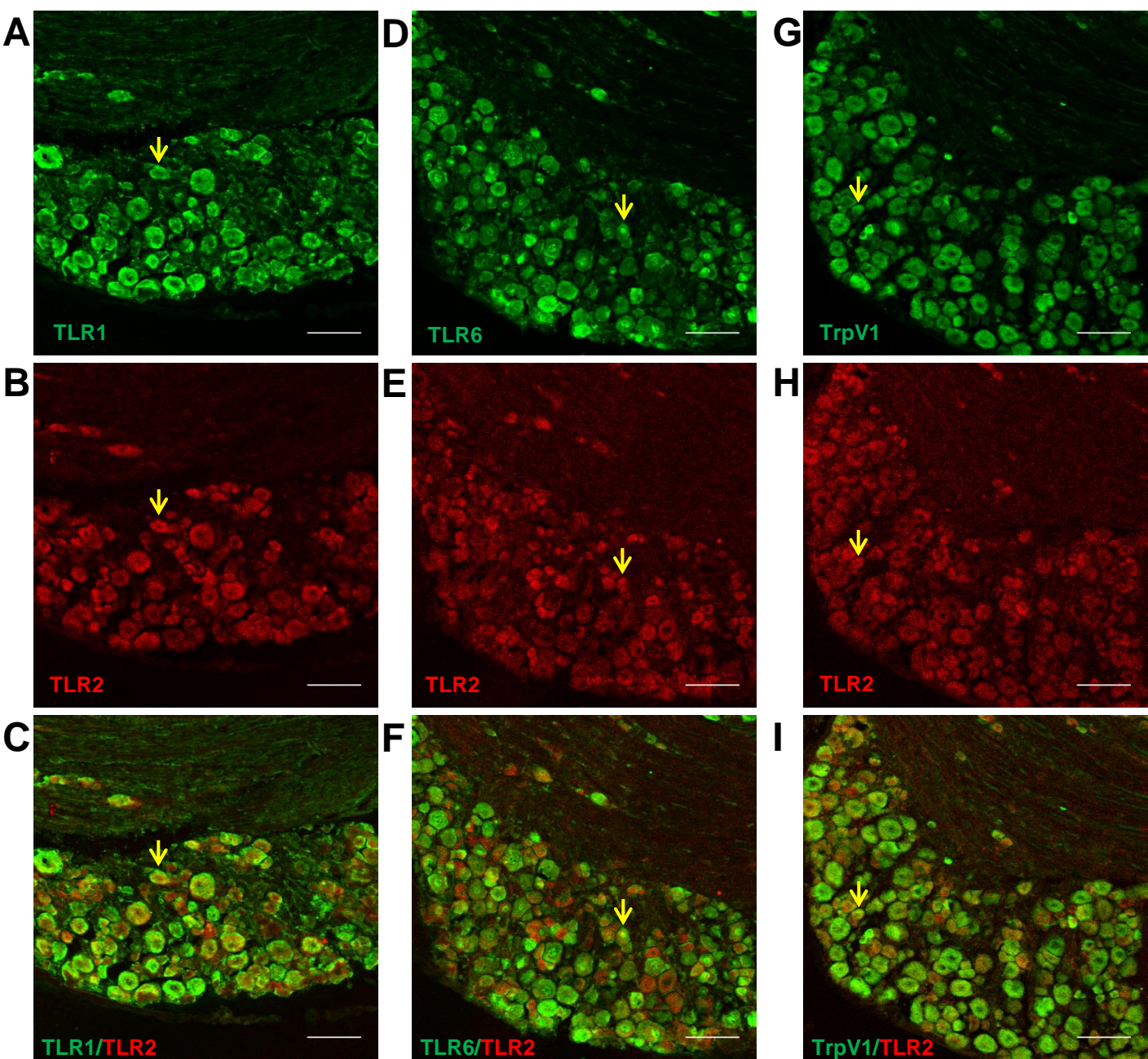


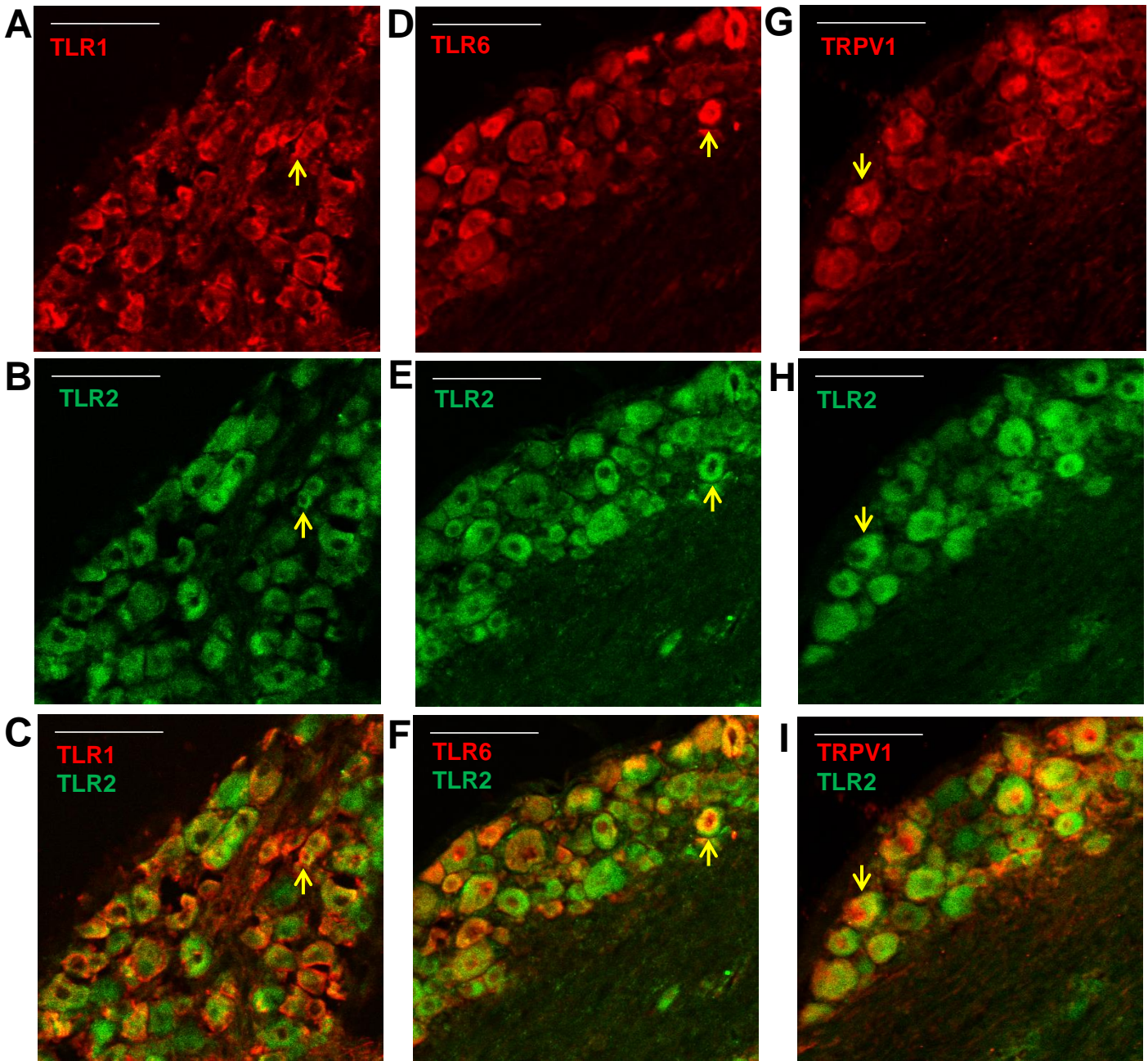
Supplementary Figure 1. (A) Representative trace (n=71 neurons) showing $[\text{Ca}^{2+}]_i$ increases in a wild-type dorsal root ganglion (DRG) neuron in response to 32-mer peptide (3 μM); Capsaicin (10 μM) and potassium (50 mM) were used as controls. (B) Histogram showing areas of neurons (in μm^2) responding to 32-mer peptide relative to the areas of all imaged neurons. (C) Representative trace showing $[\text{Ca}^{2+}]_i$ increases in a wild-type DRG neuron (n=9 neurons) in response to Pam3CSK4 (1 $\mu\text{g}/\text{mL}$); Capsaicin (10 μM) and potassium (50 mM) were used as controls. (D) Representative trace showing $[\text{Ca}^{2+}]_i$ increase in a naïve Pirt-GCaMP3 DRG neuron (n=12 neurons) within an intact DRG (*ex vivo* imaging) in response to 32-mer peptide (10 μM), but not to vehicle or to scrambled peptide (10 μM). Capsaicin (10 μM) and potassium (50 mM) were used as controls.



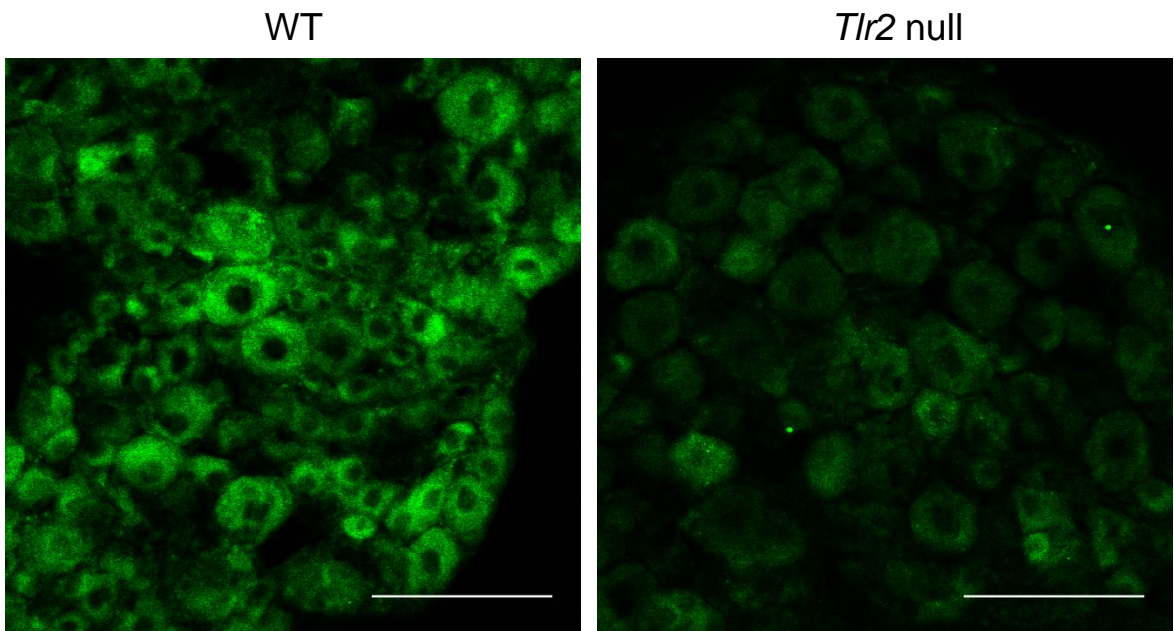
Supplementary Figure 2. Wild-type dorsal root ganglion (DRG) cells were stimulated with 10 μ M synthetic 32-mer or were unstimulated for 30 min, 1 h, 2 h, 4 h, 6 h, or 24 h (n=3-4 culture wells per condition per time point). CCL2 protein produced by the cells was measured in the conditioned medium by ELISA. At each time point, unpaired two-tailed Student's t-tests assuming equal variances; ** $p < 0.01$, * $p < 0.05$. mean \pm SEM



Supplementary Figure 3. Representative sections demonstrating expression of **(A)** TLR1, **(B, E, H)** TLR2, **(D)** TLR6, and **(G)** TrpV1 by dorsal root ganglion neurons in wild-type naïve mice (n=5). Expression of TLR2 co-localized with expression of **(C)** TLR1, **(F)** TLR6, and **(I)** Trpv1 in a subset of neurons. Examples of co-localization are indicated by arrows. Scale bar = 100 μ m.



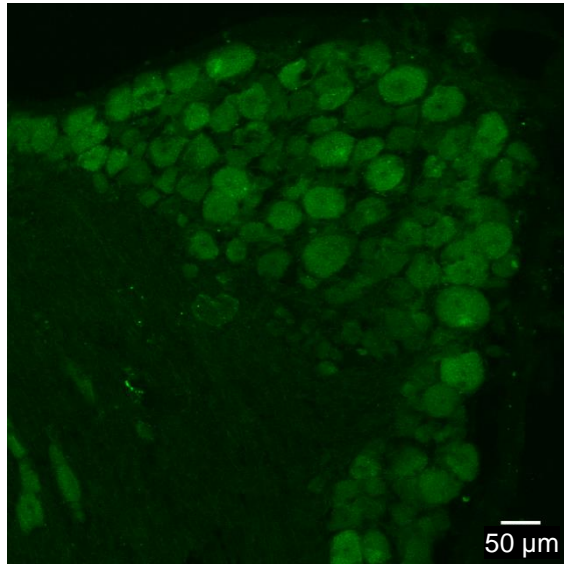
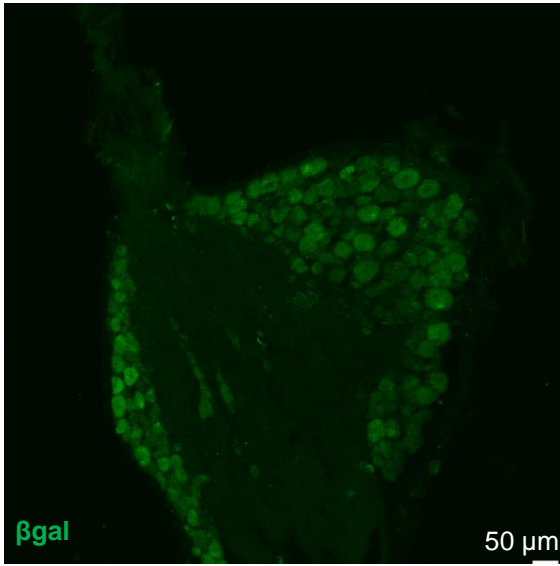
Supplementary Figure 4. An independent set of wild-type naïve mice (n=3) were used to obtain higher magnification representative sections demonstrating expression of **(A)** TLR1, **(D)** TLR6, **(G)** TRPV1, and **(B,E,H)** TLR2 by dorsal root ganglion neurons. Expression of TLR2 co-localized with expression of **(C)** TLR1, **(F)** TLR6, and **(I)** TRPV1 in a subset of neurons. Examples of co-localization are indicated by arrows. Scale bar = 100 μ m.



Supplementary Figure 5. Representative sections demonstrating specificity of TLR2 immunohistochemistry staining in L4 dorsal root ganglion neurons in **(A)** wild-type (WT) mice and not in **(B)** *Tlr2* null mice (n=3). Scale bar = 100 μ m.

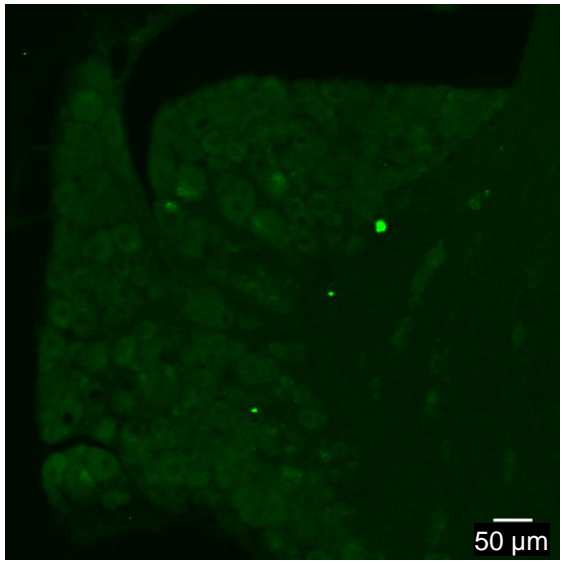
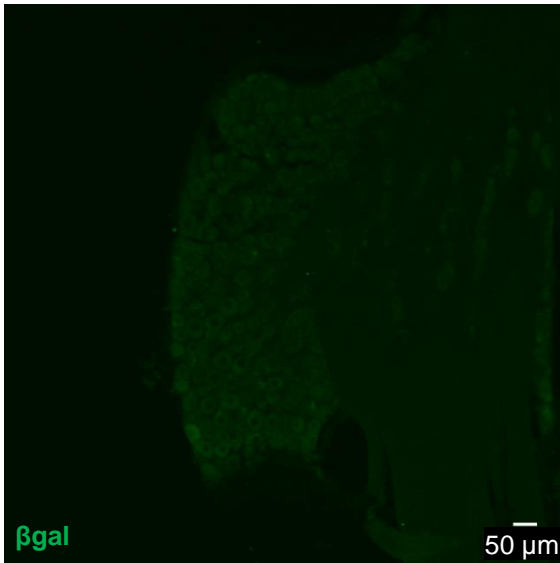
A TLR2-lacZ^{+/-} reporter – 10x

TLR2-lacZ^{+/-} reporter – 20x

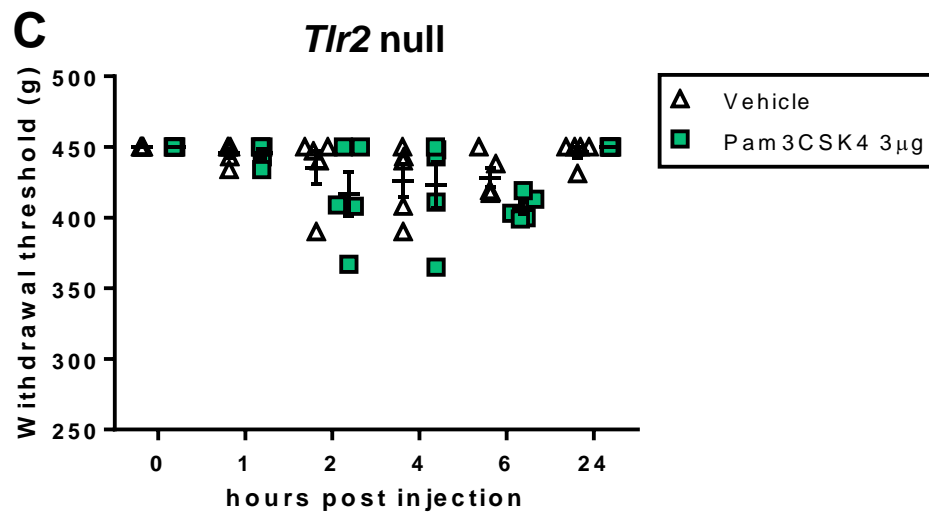
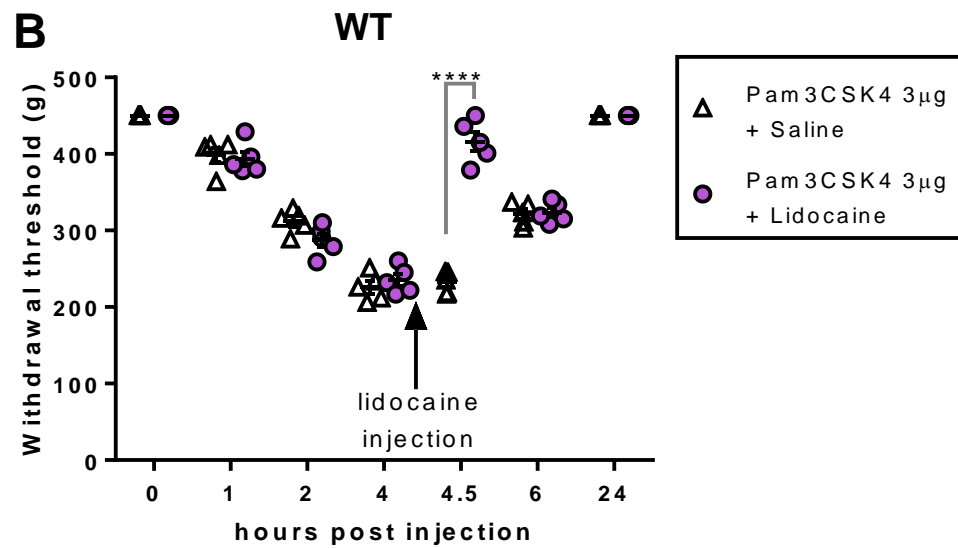
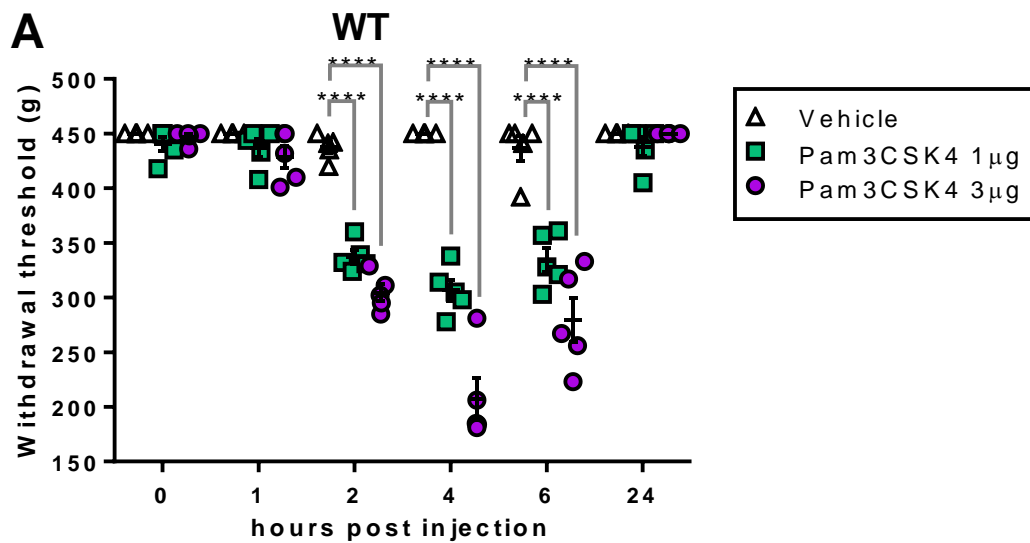


B WT – 10x

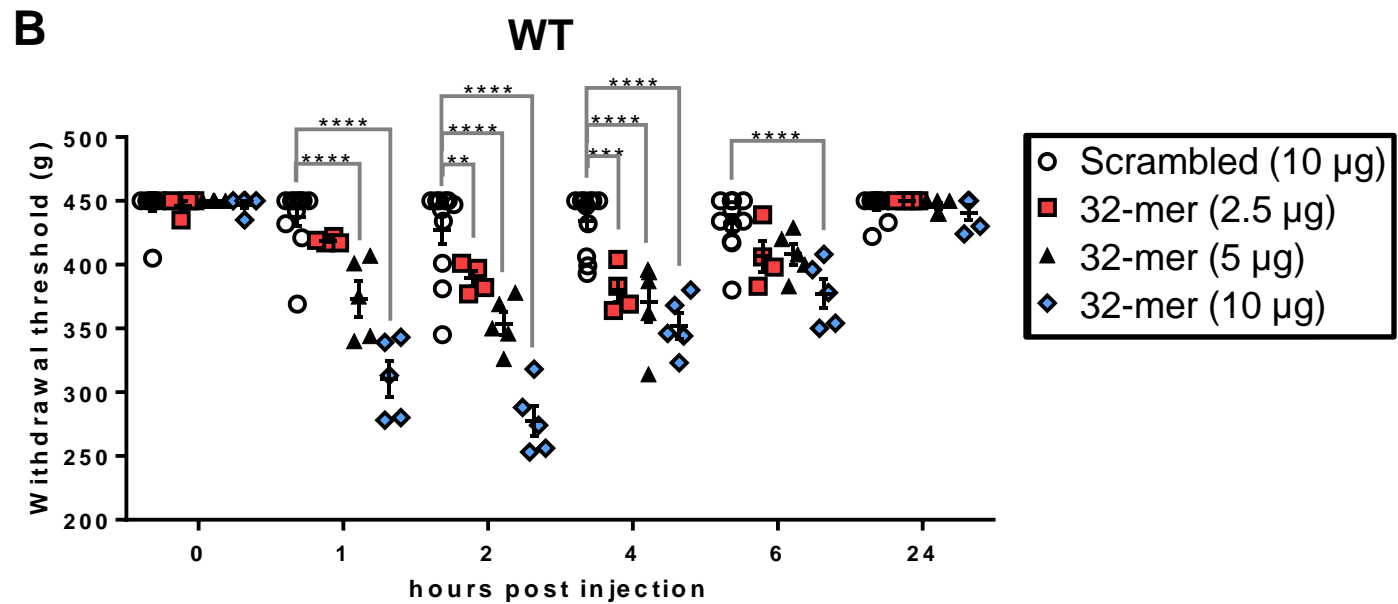
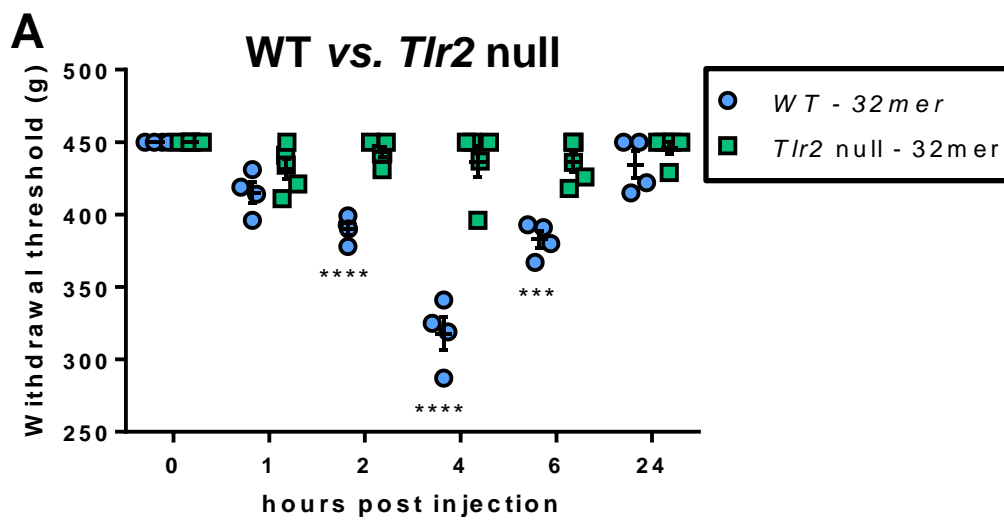
WT – 20x



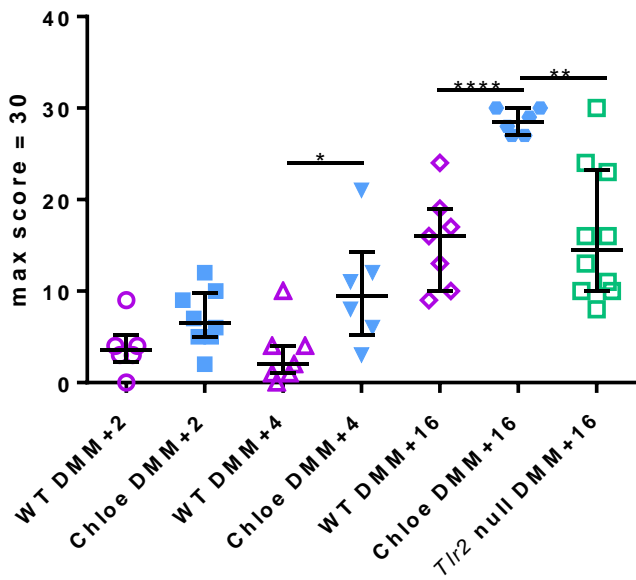
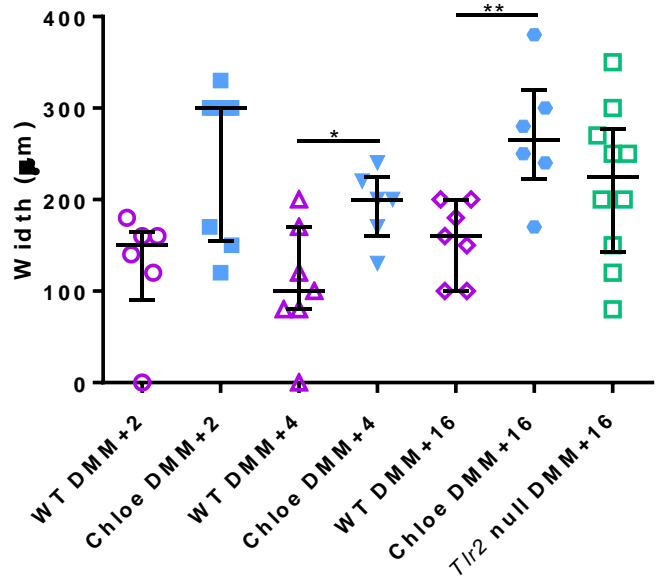
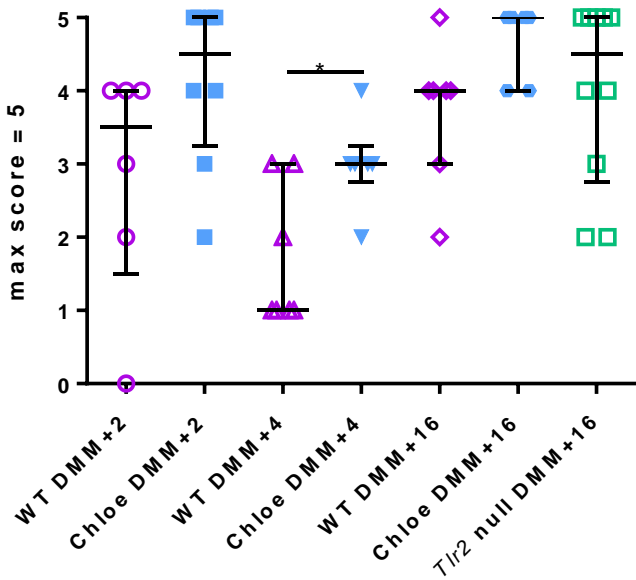
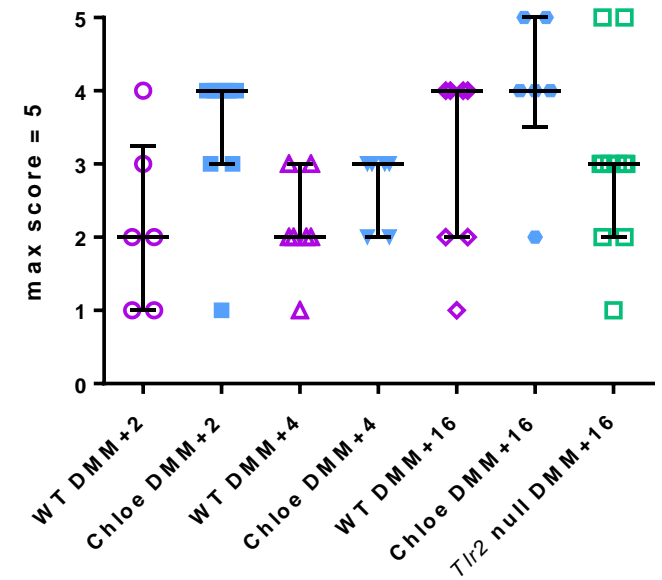
Supplementary Figure 6. β -galactosidase staining of an L4 dorsal root ganglion from **(A)** a naïve *Tlr2-lacZ^{+/-}* reporter mouse, or **(B)** a naïve wild-type (WT) mouse. Scale bar = 50 μ m.



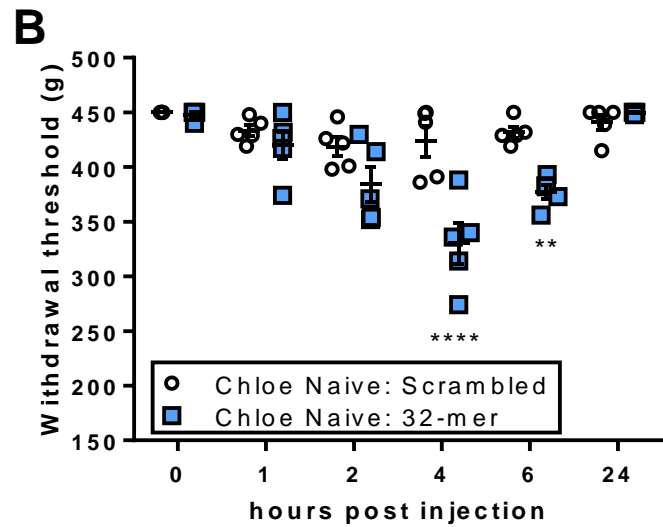
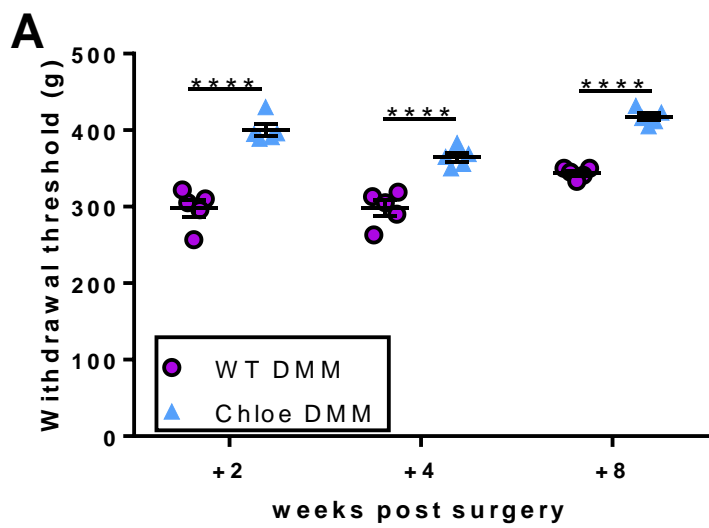
Supplementary Figure 7. Independent replicates of experiments shown in Figure 2. **A)** Intra-articular injection of vehicle, 1 or 3 μ g Pam3CSK4 in wild-type mice. $n=5$ mice/treatment. **B)** Intra-articular injection of 3 μ g Pam3CSK4 in wild-type mice followed by a second intra-articular injection of vehicle or lidocaine (20 mg/kg). $n=5$ mice/treatment. **C)** Intra-articular injection of vehicle or 3 μ g Pam3CSK4 in *Tlr2*^{-/-} mice. $n=5$ /treatment. For parts A-C: repeated measures two-way ANOVA with Bonferroni post-tests was used to compare groups at each time point **** $p<0.0001$; mean \pm SEM.



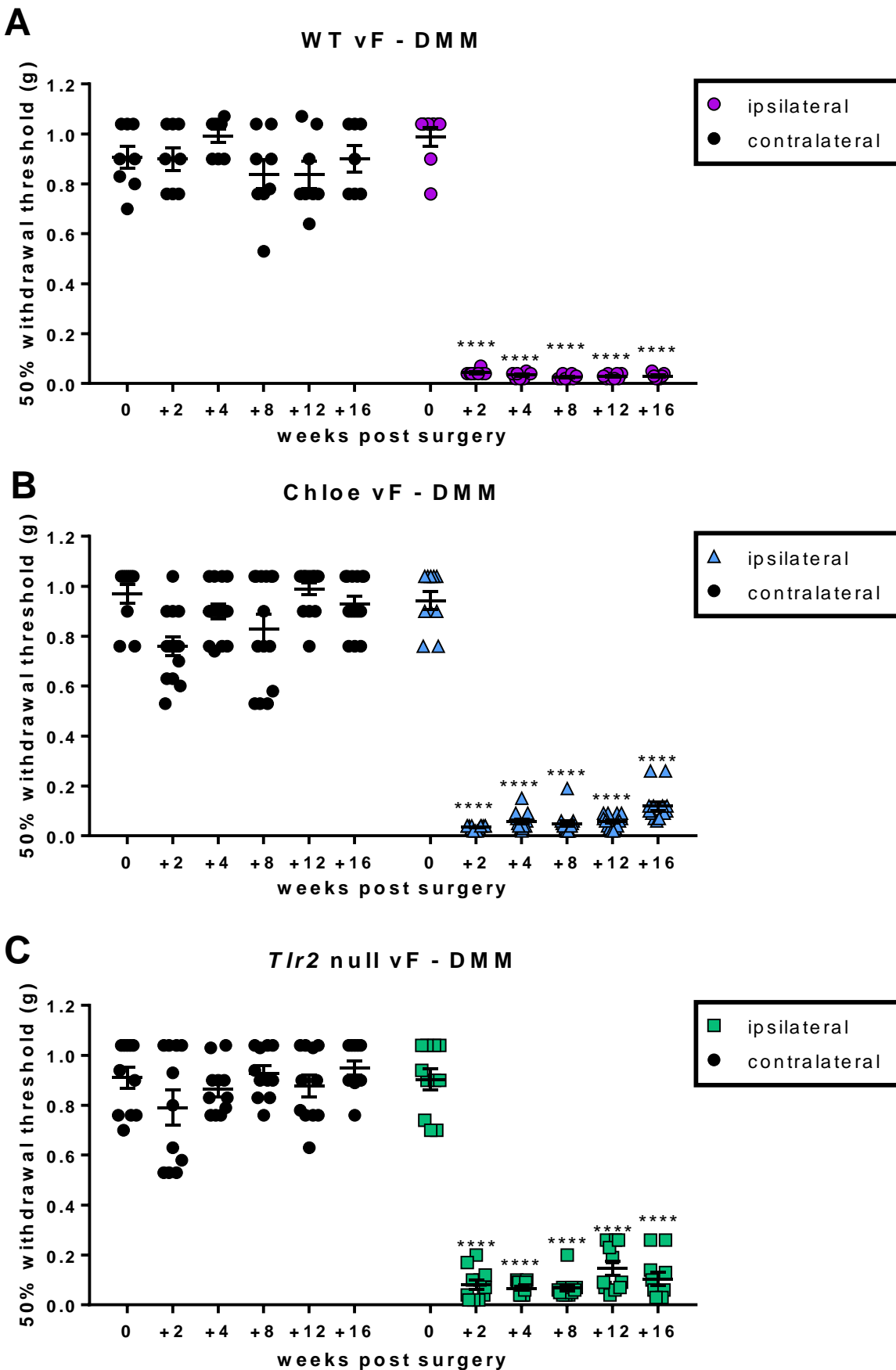
Supplementary Figure 8. Independent replicates of experiments shown in Figure 3. **A)** Intra-articular injection of 10.5 µg synthetic 32-mer peptide in wild-type (n=4) or *Tlr2*^{-/-} mice (n=5). **B)** Intra-articular injection of 2.5, 5, or 10 µg synthetic 32-mer or 10 µg scrambled peptide in wild-type mice. n=11/scrambled; n=4/32-mer (2.5 µg); n=5/32-mer (5 µg); n=5/32-mer (10 µg). For parts A-B: Repeated measures two-way ANOVA with Bonferroni post-tests was used to compare groups at each time point ***p<0.001, ****p<0.0001; mean±SEM.

A Medial Cartilage Degeneration**B** Medial Osteophyte Width**C** Bone Score**D** Synovitis

Supplementary Figure 9. Ipsilateral knee joint histological changes following destabilization of the medial meniscus (DMM) surgery in wild-type (WT), Chloe, and *Tlr2*^{-/-} mice. **(A)** Medial cartilage degeneration score, **(B)** medial osteophyte width, **(C)** subchondral bone score, and **(D)** synovitis score. For part A: WT and Chloe groups were compared using two-way ANOVA with Bonferroni post-tests at each time point; At the +16 time point, groups were compared to *Tlr2*^{-/-} were compared by Kruskal-Wallis test with Dunn's multiple comparisons test. For part B: Data were log-transformed before WT and Chloe groups were compared using two-way ANOVA with Bonferroni post-tests at each time point; At the +16 time point, groups were compared to *Tlr2*^{-/-} were compared by one-way ANOVA with Bonferroni post-tests. For parts C-D: WT and Chloe groups were compared at each time point by Mann-Whitney test; At the +16 time point, groups were compared to *Tlr2*^{-/-} were compared by Kruskal-Wallis test with Dunn's multiple comparisons test. For parts A-D: *p<0.05, **p<0.01, ****p<0.0001. median \pm IQR.



Supplementary Figure 10. Independent replicates of experiments shown in Figure 4. **A)** Time course of knee hyperalgesia in wild-type (n=5) vs. Chloe (n=5 mice) after destabilization of the medial meniscus (DMM) surgery. **B)** Intra-articular injection of 10.5 μ g synthetic 32-mer or scrambled peptide in naïve Chloe mice. n=5/group. For parts A-B: Repeated measures two-way ANOVA with Bonferroni post-tests was used to compare groups at each time point. **p<0.01, ****p<0.0001; mean \pm SEM.



Supplementary Figure 11. (A) Wild-type (WT), **(B)** Chloe, and **(C)** *Tlr2*^{-/-} mice develop ipsilateral mechanical allodynia (n=8-14 mice/time point) through 16 weeks post destabilization of the medial meniscus (DMM) surgery. For parts A-C: one-way ANOVA with Bonferroni post-tests was used to compare each time point to time 0; ****p<0.0001 vs time 0. mean±SEM.

Supplemental Methods

Animals and surgery: All animal experiments were approved by the Institutional Animal Care and Use Committees at Rush University Medical Center. Animals were housed with food and water *ad libitum* and kept on 12-hour light cycles. Wild-type C57BL/6 mice, *Tlr2-lacZ*^{+/-} reporter mice (*Tlr2*^{tm1(KOMP)Vlcg} Targeting Project: VG15097 from UC Davis KOMP repository), Chloe mice (C57BL/6 background), *Tlr2*^{-/-} mice (Jackson, C57BL/6 background), *Tlr4*^{-/-} mice (Jackson, C57BL/6 background), and Pirt-GCaMP3 mice (courtesy of Dr. Xinzhong Dong, Johns Hopkins University, Baltimore, MD, C57BL/6 background (1)) were used. All numbers of mice used are outlined in the figure legends. DMM or sham surgery was performed as previously described (2, 3) in the right knee of 10-week old male mice. Briefly, after medial parapatellar arthrotomy, the anterior fat pad was dissected to expose the anterior medial meniscotibial ligament, which was severed. The knee was flushed with saline and the incision closed.

Reagents: Synthetic mouse 32-mer (FFGVGGEDDITIQTVTWPDLELPLPRNVTEGE) and scrambled peptide (LPTFGEVEVWLLGEDQDFDIPTTVGPRTGEIN) (no known homology to any protein) were purchased from Auspep (Tullamarine, Australia) or from David Jackson (University of Melbourne, Melbourne, Australia). Endotoxin levels were confirmed to be <0.01 EU/μg by LAL assay (Fisher Scientific, Pittsburgh, PA). Native, glycosylated 32-mer peptide was isolated from pig articular cartilage, as described previously (4).

DRG cell culture and stimulations: Cells were isolated from knee-innervating dorsal root ganglia (L3-L5) of 3-4 mice (male or female naïve C57BL/6, *Tlr2*^{-/-}, or *Tlr4*^{-/-}) mice at least 10 weeks of age), plated onto glass coverslips, and cultured in adult neurogenic medium, as previously described (3). Overnight stimulations from days 3-4 were carried out with 32-mer peptide (0.3-30 μM), scrambled peptide, native 32-mer (10 μM), or synthetic TLR2 ligand Pam3CSK4 (Invivogen, 1 μg/mL). Experiments with native 32-mer were carried out in the presence of polymyxin B (30 μg/mL, Sigma-Aldrich, St. Louis, MO). Supernatants were collected for protein analysis. Figure legends indicate the number of independent culture experiments conducted for each type of stimulation.

Protein analysis of supernatant: Total protein levels were determined by BCA assay (Thermo Fisher Scientific, Inc., Rockford, IL), and CCL2 protein levels were determined via ELISA (R&D Systems Inc, Minneapolis, MN).

In vitro calcium imaging: The response of cultured DRG neurons (as described above) to selected DAMPs was recorded through intracellular Ca^{2+} -imaging, following standard protocols using Fura-2AM (2 μ M; Life Technologies, Grand Island, NY) and a balanced salt solution (BSS) (140 mM NaCl, 10 mM HEPES, 2 mM $CaCl_2 \cdot 2H_2O$, 1 mM $MgCl_2 \cdot 6H_2O$, 5 mM KCl, 10 mM glucose) (3, 5). 32-mer peptide (3-10 μ M), scrambled peptide (3 μ M), or Pam3CSK4 (1 μ g/mL) was applied for 3 min by adding 0.5 mL of solution to the bath chamber. Cells were washed with balanced salt solution before applying controls (potassium (50 mM) and capsaicin (10 μ M)).

Ex vivo calcium imaging of intact DRG: Three intact DRG explants (one L3, two L4) were isolated from a naïve 14-week old male Pirt-GCaMP3 mouse. These mice express the fluorescent calcium indicator, GCaMP3, in ~90% of all sensory DRG neurons, and not in other peripheral or central tissues, through the Pirt promoter. Intact DRG were equilibrated on ice in BSS, as above. After 30 minutes, explants were placed in a perfusion chamber within BSS and imaged using a Zeiss Axio Observer D1 fluorescent microscope (Carl Zeiss Microscopy, LLC, Thornwood, NY) at 10x magnification, 0.5 Hz, and using a Zeiss GFP filter set (excitation: 450-490 nm, emission: 500-550 nm) (6). Briefly, explants were stimulated by perfusing the chamber with 2 mL of BSS solution containing 10 μ M 32-mer peptide, 10 μ M scrambled peptide, or BSS solution alone. Positive controls (potassium and capsaicin) were applied as for in vitro calcium imaging. Image analysis was performed using an ImageJ (7) macro to determine change in fluorescence intensity with time.

Immunofluorescence for TLRs: Naïve wild-type mice (12-16 weeks of age, n=5; 19 weeks of age, n=3) or naïve *Tlr2*^{-/-} mice (14 weeks of age, n=3) were anesthetized by ketamine and xylazine and perfused transcardially with PBS followed by 4% paraformaldehyde in PBS. The spinal column was dissected and postfixed in 4% paraformaldehyde overnight followed by cryopreservation in 30% sucrose in PBS. L4 DRGs were embedded with OCT (Tissue-Tek), frozen with dry ice, and cut into 12 μ m sections. For immunostaining, slides were allowed to dry at room temperature for 1 h, postfixed with 4% paraformaldehyde for 10

min, and washed with PBS. Sections were blocked and permeabilized with 5% normal goat serum in 0.1% triton in PBS prior to incubation with primary antibodies. Sections were stained with TLR2 rat monoclonal antibody (Abcam; ab11864) in conjunction with TLR1 (Abcam; ab37068), TLR6 (Abcam; ab37072) or TrpV1 (Abcam; ab31895) rabbit polyclonal antibodies overnight at 4 °C; sections were washed with PBS and incubated with appropriately conjugated AlexaFluor 488 and AlexaFluor 633 antibodies (Invitrogen #A11006 and #A21070, 1:500) for 1 h at room temperature. TLR2-lacZ reporter mice were stained with β -galactosidase rabbit polyclonal antibody (Molecular Probes; A-11132) overnight at 4 °C; sections were washed with PBS and incubated with goat anti-rabbit AlexaFluor 488 antibody (Invitrogen #A11006, 1:500) for 2 h at room temperature. Lastly, the sections were washed with PBS and mounted with Vectashield mounting media. Fluorescent signals were captured using a confocal microscope, and the images were analyzed using ImageJ and Photoshop. For quantification, three sections per DRG were used and the number of neurons that co-expressed TLR2 with TLR1, TLR6 or TRPV1 were summed across the 3 sections and normalized to the total number of DRG neurons (phase contrast images) summed across the 3 sections.

Immunofluorescence for LacZ: One wild-type and one *Tlr2-lacZ^{+/-}* reporter mouse (male, 10 weeks of age) were anesthetized by ketamine and xylazine and perfused transcardially with PBS followed by 4% paraformaldehyde in PBS. The spinal column was dissected and postfixed in 4% paraformaldehyde overnight followed by cryopreservation in 30% sucrose in PBS. Ipsilateral L4 DRG were embedded with OCT (Tissue-Tek), frozen with dry ice, and cut into 12 μ m sections. For immunostaining, slides were allowed to dry at room temperature for 1 h and washed with PBS. Sections were blocked and permeabilized with 5% normal goat serum in 0.1% triton in PBS prior to incubation with primary antibodies. Sections were stained with β -galactosidase rabbit polyclonal antibody (Molecular Probes; A-11132) overnight at 4 °C; sections were washed with PBS and incubated with goat anti-rabbit AlexaFluor 488 antibody (Invitrogen #A11006, 1:500) for 2 h at room temperature. Lastly, the sections were washed with PBS and mounted with Vectashield mounting media. Fluorescent signals were captured using a confocal microscope, and the images were analyzed using ImageJ and Photoshop.

Knee hyperalgesia: Knee hyperalgesia was measured in wild-type, Chloe, and *Tlr2*^{-/-} mice using a Pressure Application Measurement (PAM) device (Ugo Basile, Varese, Italy) as previously described (8-10). Briefly, mice were restrained by hand and the hind paw was lightly pinned with a finger in order to hold the knee in flexion at a similar angle for each mouse. With the knee in flexion, the PAM transducer was pressed against the medial side of the ipsilateral knee while the operator's thumb lightly held the lateral side of the knee. The PAM software guided the user to apply an increasing amount of force at a constant rate (30 g/s), up to a maximum of 450 g. If the mouse tried to withdraw its knee, the force at which this occurred was recorded. If the mouse did not try to withdraw, the maximum possible force of 450 g was assigned. Two measurements were taken per knee and the withdrawal force data were averaged. The operator was blinded to treatment.

Intra-articular injection: Under isoflourane anesthesia, a 30 gauge needle and Hamilton syringe were used to inject 3 μ L of Pam3CSK4 (1 or 3 μ g dissolved in sterile H₂O), lidocaine (20 mg/kg in saline), 32-mer or scrambled peptide (10.5 μ g in PBS), or vehicle (3 μ L) through the patellar tendon and into the intra-articular space of the right knees of mice.

Histopathology of the knee: Sixteen weeks after DMM, histopathology of the knee was evaluated based on OARSI recommendations (11) (Alison Bendele, Bolder BioPATH, Inc., Boulder CO). Joints were fixed in 10% formalin, decalcified, embedded in the frontal plane, sectioned, and stained with Toluidine blue, as described (3). In this model of osteoarthritis, damage develops in the medial compartment (12). Medial femoral condyles and tibial plateaux were scored for severity of cartilage degeneration. For each cartilage surface, scores were assigned individually to each of 3 zones (inner, middle, outer) on a scale of 0-5, with 5 representing the most damage. Therefore, the maximum summed score = 30. The largest osteophyte (medial tibia or femur) was measured using an ocular micrometer. The extent of subchondral bone sclerosis/reduction in bone marrow area was scored from 0 to 5, where 0=no increase; 1=minimal (1-10% increase in bone mass/trabecular widths); 2=mild (11-25% increase in bone mass/trabecular widths); 3=moderate (26-50% increase in bone mass/trabecular widths); 4=marked (51-75% increase in bone mass/trabecular widths); and 5=severe (>75% increase in bone mass/trabecular widths). Synovial changes (inflammation and/or fibrosis) were scored from 0 to 5, where 0 = normal and 5 = severe.

Mechanical allodynia: Wild-type, Chloe, and *Tlr2*^{-/-} mice were tested for secondary mechanical allodynia of the ipsilateral hind paw using von Frey fibers and the up-down staircase method, as previously described (13). Withdrawal thresholds were assessed before surgery and weeks 2, 4, 8, 12, and 16 after DMM.

References

1. Kim YS, Chu Y, Han L, Li M, Li Z, Lavinka PC, Sun S, Tang Z, Park K, Caterina MJ, et al. Central terminal sensitization of TRPV1 by descending serotonergic facilitation modulates chronic pain. *Neuron*. 2014;81(4):873-87.
2. Glasson SS, Blanchet TJ, and Morris EA. The surgical destabilization of the medial meniscus (DMM) model of osteoarthritis in the 129/SvEv mouse. *Osteoarthritis Cartilage*. 2007;15(9):1061-9.
3. Miller RE, Tran PB, Das R, Ghoreishi-Haack N, Ren D, Miller RJ, and Malfait AM. CCR2 chemokine receptor signaling mediates pain in experimental osteoarthritis. *Proc Natl Acad Sci U S A*. 2012;109(50):20602-7.
4. Fosang AJ, Last K, Poon CJ, and Plaas AH. Keratan sulphate in the interglobular domain has a microstructure that is distinct from keratan sulphate elsewhere on pig aggrecan. *Matrix Biol*. 2009;28(1):53-61.
5. Oh SB, Tran PB, Gillard SE, Hurley RW, Hammond DL, and Miller RJ. Chemokines and glycoprotein120 produce pain hypersensitivity by directly exciting primary nociceptive neurons. *J Neurosci*. 2001;21(14):5027-35.
6. Miller RE, Belmadani A, Ishihara S, Tran PB, Ren D, Miller RJ, and Malfait AM. Damage-associated molecular patterns generated in osteoarthritis directly excite murine nociceptive neurons through Toll-like receptor 4. *Arthritis & rheumatology*. 2015;67(11):2933-43.
7. Schneider CA, Rasband WS, and Eliceiri KW. NIH Image to ImageJ: 25 years of image analysis. *Nat Methods*. 2012;9(7):671-5.
8. Barton NJ, Strickland IT, Bond SM, Brash HM, Bate ST, Wilson AW, Chessell IP, Reeve AJ, and McQueen DS. Pressure application measurement (PAM): a novel behavioural technique for measuring hypersensitivity in a rat model of joint pain. *J Neurosci Methods*. 2007;163(1):67-75.
9. Leuchtweis J, Imhof AK, Montechiaro F, Schaible HG, and Boettger MK. Validation of the digital pressure application measurement (PAM) device for detection of primary mechanical hyperalgesia in rat and mouse antigen-induced knee joint arthritis. *Methods Find Exp Clin Pharmacol*. 2010;32(8):575-83.
10. Miller RE, Ishihara S, Bhattacharyya B, Delaney A, Menichella DM, Miller RJ, and Malfait AM. Chemogenetic Inhibition of Pain Neurons in a Mouse Model of Osteoarthritis. *Arthritis and rheumatism*. In press.
11. Glasson SS, Chambers MG, Van Den Berg WB, and Little CB. The OARSI histopathology initiative - recommendations for histological assessments of osteoarthritis in the mouse. *Osteoarthritis Cartilage*. 2010;18 Suppl 3(S17-23).
12. Miller RE, Tran PB, Ishihara S, Larkin J, and Malfait AM. Therapeutic effects of an anti-ADAMTS-5 antibody on joint damage and mechanical allodynia in a murine model of osteoarthritis. *Osteoarthritis and cartilage / OARS, Osteoarthritis Research Society*. 2016;24(2):299-306.

13. Miller RE, Tran PB, Das R, Ghoreishi-Haack N, Ren D, Miller RJ, and Malfait AM. CCR2 chemokine receptor signaling mediates pain in experimental osteoarthritis. *Proceedings of the National Academy of Sciences of the United States of America*. 2012;109(50):20602-7.